

Quasi-1d quantum helimagnets: The fate of multipolar phases

S. Nishimoto,¹ S.-L. Drechsler*,¹ R. Kuzian,¹ J. Richter,² and J. van den Brink¹

¹IFW Dresden, P.O. Box 270116, D-01171 Dresden, Germany

²Universität Magdeburg, Institut für Theoretische Physik, Germany

(Dated: October 17, 2018)

Coupled frustrated spin-1/2 chains in high magnetic fields described within the ferro- antiferromagnetic J_1 - J_2 Heisenberg model are studied by DMRG, hard core boson, and spin wave theory approaches. Multipolar phases related to magnon bound states are destroyed (supported) by weak antiferromagnetic (ferromagnetic) interchain couplings J_{ic} . We show that quantum spin nematics might be found for LiVCuO_4 whereas for $\text{Li}(\text{Na})\text{Cu}_2\text{O}_2$ it is prevented by a sizeable antiferromagnetic J_{ic} . Also for $\text{Li}_2\text{ZrCuO}_4$ with a small antiferromagnetic J_{ic} expected triatic or quartic phases are unlikely, too. The saturation field is found to be strongly affected even by a relatively small J_{ic} .

The frustration of magnetic interactions allows for new phenomena to emerge. Some spin-chain compounds are frustrated magnets in, for instance, the case of ferromagnetic (FM) nearest neighbor (NN) exchange interaction (J_1) competing with an antiferromagnetic (AFM) next-neighbor (NNN) one (J_2) [2]. Recent theoretical studies indicate that in a high magnetic field, such a J_1 - J_2 chain can display e.g. nematic quasi long-range order for certain $\alpha = -J_2/J_1$ [3–5]. This nematic state might be thought of as a condensate of two-magnon bound states [6]. Depending on the value of α also three- or four- magnon boundstates might condense, resulting in a very rich phase diagram with exotic magnetic multipolar (MMP) phases. However, to establish whether these MMP phases can be realized in a real material it is essential to determine their robustness, i.e. the very existence of multimagnon bound states (MBS) with respect to various interchain (IC) couplings J_{ic} , which can be (very) small for certain spin-chain compounds, but that is always present, and, as we will show here can be detrimental. Such a transition from 1D to 2D or 3D can be non-trivial. In particular, from quantum mechanics it is well-known that bound states are strongly pronounced in 1D and more rare in 2D or 3D. To understand *quantitatively* the role of IC the question arises in which cases even a relatively weak IC is still important or even crucial? Here we address such a problem, namely, the fate of MMP states, such as the nematic spin state related to MBS at high magnetic fields and consider the spin-1/2 frustrated isotropic J_1 - J_2 -Heisenberg model mentioned above supplemented by various IC [7]. Recently, the 1D-model and related compounds revealed considerable interest [2, 8–22]. Nowadays it is the most popular model for edge-shared chain cuprates (see e.g. [2]). Additional AFM couplings typically provided by the IC enhance the kinetic energy of magnons. Hence, AFM(FM) IC may hinder(favor) the formation of low-lying MBS. A FM IC may create even new MMP states. An examination of real Q-1D systems to predict the changes due to finite J_{ic} and to evaluate the chances to detect MMP states in certain compounds is of broad interest [6, 16–20, 23–26].

Among edge-shared cuprates LiCu_2O_2 , the isomor-

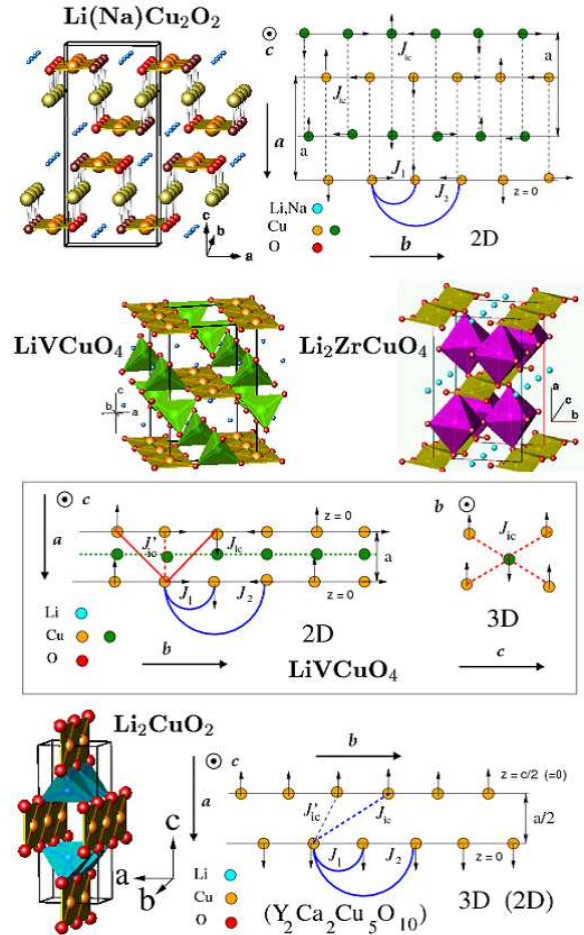


FIG. 1: (Color) Crystal structure and exchange patterns of chain cuprates. The main in- and interchain exchange paths are marked by arcs and lines, respectively. Upper: 1/2-unit cell projection (right). Planes with green and yellow Cu sites are treated as uncoupled. We take into account only perpendicular inplane J_{ic} . Middle: The main 2D IC in the basal plane of unshifted chains (left) and with 3D IC (right). Lower: Two NN shifted chains in different (ab)-planes. We ignore the weak J'_{ic} and keep only the second diagonal J_{ic} [17].

phic NaCu_2O_2 , and $\text{LiVCuO}_4 \equiv \text{LiCuVO}_4$ [27] (see Fig. 1; for comparison the reference systems Li_2CuO_2 and $\text{Ca}_2\text{Y}_2\text{Cu}_5\text{O}_{10}$ with strong IC are shown, too) have been proposed to be candidates for quantum-spin nematics, i.e. quadrupolar phases derived from 2-MBS. Systems like $\text{Li}_2\text{ZrCuO}_4$ [12, 22] located closer to the FM-spiral critical point might be candidates for the triatic or quartic MMP. Besides the strength also the influence of various IC topologies resulting from different arrangements of individual chains is of interest. Various types of IC are shown in Fig. 1. The simplest case is given by unshifted neighboring chains and a predominant perpendicular J_{ic}^\perp . Here spirals on NN chains are only weakly affected by an AFM IC [16] (classically their pitch angle, i.e. the incommensurate (INC) inchain magnetic structure in the dipolar phase at ambient external fields remains even unaffected). Hereafter, we call this IC the 'unfrustrated IC'. An effective 2D arrangement of the magnetically active Cu^{2+} -sites is realized approximately for $\text{Li}(\text{Na})\text{Cu}_2\text{O}_2$, where $J_{\text{ic}} \sim (0.5 \text{ to } 1)J_2 \sim 40 \text{ to } 100 \text{ K}$ [28–30]. A square lattice of unshifted chains, i.e. the 3D case considered in Ref. 24 might be realized in LiVCuO_4 , if the IC denoted as J_3 in Ref. 25 is dominant as compared with the IC in the (ab) -plane (see middle of Fig. 1). Another 3D case but with shifted adjacent chains is realized for Li_2CuO_2 (see Fig. 1) for which H_s has been found recently [18]. $J_{\text{ic}} \approx 10 \text{ K}$ can be extracted from $H_s(0)$, from inelastic neutron scattering studies, and from bandstructure results [17]. The same order holds also for $\text{Li}_2\text{ZrCuO}_4$ where buckling of the CuO_2 chains reduces J_{ic} [14].

We used the density-matrix renormalization group (DMRG) method [31] with imposing periodic boundary conditions (PBC) for all directions. In general, it is known that this method is much less appropriate for $D > 1$. However, spin systems with up to about $\sqrt{n} \times \sqrt{n} \times L = \sqrt{10} \times \sqrt{10} \times 50$ sites can be studied by taking a proper construction of the lattice block (see Ref. 18). We kept $m \approx 800 - 4000$ density-matrix eigenstates in the renormalization procedure. In fact, about 100 – 300 sweeps are necessary to obtain the GS energy within a convergence of $10^{-7}J_1$ for each m value. All calculated quantities were extrapolated to $m \rightarrow \infty$ and the maximum error in the GS energy is estimated as $\Delta E/J_1 \sim 10^{-4}$, while the discarded weight is less than 1×10^{-6} . Under the PBC, a uniform distribution of $\langle S_i^z \rangle$ may give an indication to examine the accuracy of DMRG calculations for spin systems. Typically, $\langle S^z \rangle - S_{\text{tot}}^z/(nL)$ is less than 1×10^{-3} in our calculations. Note that for high-spin states [$S_{\text{tot}}^z \gtrsim (nL - 10)/2$] the GS energy can be obtained with an accuracy of $\Delta E/J_1 < 10^{-12}$ by carrying out several thousands sweeps even with $m \approx 100 - 800$. Furthermore, we studied the systems with several lengths: $L = 16 - 64$ (24 – 96) for 3D (2D) and then adopting power laws we performed a finite-size-scaling analysis to obtain the saturation field $h_s \equiv g\mu_B H_s/|J_1|$ in the thermodynamic limit $L \rightarrow \infty$. As a result, we ob-

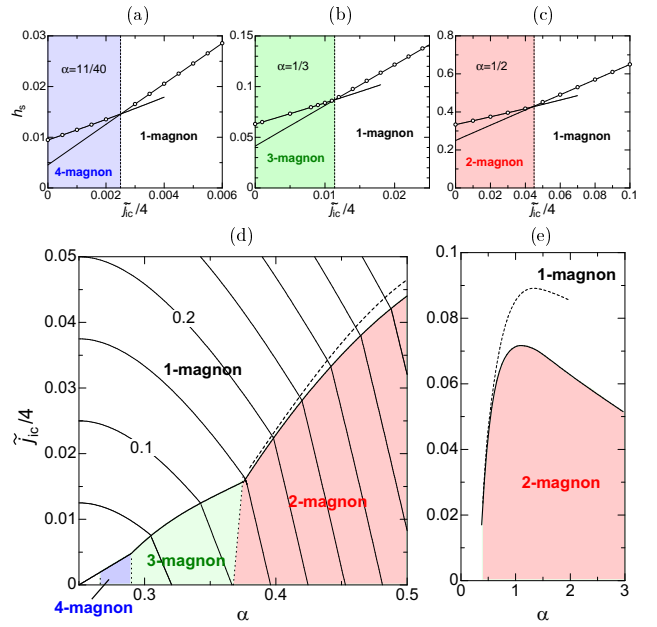


FIG. 2: (Color) Upper (a-c): Saturation field vs IC; lower: critical IC for the 3D case with perpendicular IC $\tilde{j}_{\text{ic}} = N_{\text{ic}}J_{\text{ic}}^\perp/|J_1|$ vs. inchain frustration α (d,e), where $N_{\text{ic}} = 4$ is the number of nearest interchain neighbors. The phase boundaries are constructed from the 'kinks' in h_s -plots like in (a-c). The contour lines in (d) show the values of h_s . The 2D case with $N_{\text{ic}}=2$ is shown also in (d,e) (dotted lines).

tain h_s with high accuracy. In addition to DMRG we have also applied the linear spin wave theory and the hard core boson approach [15]. The latter provides exact results for the nematic phase. Some results for the reported magnetization curves have been additionally checked applying the exact diagonalization.

We start with the simplest IC case of parallel chains within a plane (2D) or within a square-lattice arrangement of chains (3D) and a single perpendicular IC $J_{\text{ic}}^\perp = j_{\text{ic}}^\perp|J_1|$ (see Figs. 1,2). A typical magnetization curve for the nematic phase is shown in Fig. 3. The height of the magnetization steps $\Delta S^z = 2$, only, is its signature whereas in the 1-magnon phase $\Delta S^z = 1$ holds. Note that a rather weak critical IC of a few percent will remove the nematic phase in favor of the usual field induced "conic" phase. The saturation field h_s of the INC phase on the 1-magnon side is described exactly already within spin wave theory:

$$h_s \equiv g\mu_B H_s/|J_1| = 2\alpha - 1 + 0.125/\alpha + \tilde{j}_{\text{ic}}, \quad (1)$$

where $\tilde{j}_{\text{ic}} = N_{\text{ic}}j_{\text{ic}} = 2(D-1)j_{\text{ic}}$ for $D=2,3$. Using the Curie-Weiss temperature $\Theta_{\text{CW}} = -(J_1 + J_2 + 0.5N_{\text{ic}}J_{\text{ic}})/2$ which determines the high-temperature spin susceptibility $\chi(T) \sim 1/(T - \Theta_{\text{CW}})$, the IC in Eq. (1) can be eliminated. Then in this 1-magnon phase one has a simple expression to extract J_1 or α from H_s and Θ_{CW} :

$$g\mu_B H_s(J_{\text{ic}}) + 4\Theta_{\text{CW}}(J_{\text{ic}}) \equiv G = |J_1| [1 + 1/(8\alpha)]. \quad (2)$$

A relation $G = |J_1|f(\alpha)$ is valid also in other regimes, where f is a simple function affected by the type of the IC and the region of the MMP phase diagram. In the 1-magnon regimes valid for Li_2CuO_2 and $\text{Ca}_2\text{Y}_2\text{Cu}_5\text{O}_{10}$ (see below) we have $f = 2(1 - \alpha)$ [18]. For the nematic phase in full accord with the DMRG we obtained numerically *exact* values of h_s using the hard-core boson approach [15]. Expanding the 2-particle Green's function in powers of $j_{ic} \ll 1$ we arrive at analytical expressions:

$$h_s(\alpha) \approx h_s^{1D}(\alpha) + \tilde{j}_{ic}/2 + N_{ic}\eta(\alpha)j_{ic}^2 + O(j_{ic}^4), \quad (3)$$

$$h_s^{1D}(\alpha) = 2\alpha - 1 + 0.5/(1 + \alpha), \quad (4)$$

where $\eta(\alpha) = (1 + \alpha)(3\alpha^2 + 3\alpha + 1)/[2(1 + 2\alpha)^2] \approx 5/3 + 3\alpha/2$. The expansion coefficients for higher order terms differ for $D=2$ and 3 reflecting subtle natural differences in the quantum fluctuations. A detailed discussion will be given elsewhere. Comparing the Eqs. (1) and (3) we stress the presence of nonlinear IC terms and two times smaller linear term in the nematic phase as compared with the usual one-magnon phase. The inspection of Figs. 2(d,e) shows that the critical IC of the nematic region reaches a maximum as a function of α . Its position $\alpha \approx 1.103$ and height $\tilde{j}_{ic}/4 \approx 0.071688$ are close to the feature shown in Fig. 6 of Ref. 24.

Keeping the linear IC term in Eq. (3) we arrive at

$$g\mu_B H_s + 2\Theta_{CW} \equiv K = |J_1|[\alpha + 0.5/(1 + \alpha)]. \quad (5)$$

Thus, G and K composed from IC affected quantities depends itself on single chain properties, only. In most cases it is easier to determine the latter theoretically whereas G or K can be found from experiment.

Applying Eq. (2) to $\text{Li}_2\text{ZrCuO}_4$ we predict $\Theta_{CW} = 93.3$ K for a preliminary experimental value of H_s of about 13 T [32] using $J_1 = 273$ K, $\alpha = 0.29$ to 0.3

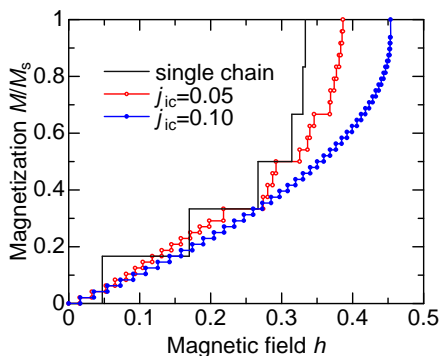


FIG. 3: (Color) Magnetization vs. applied external field for a 2D arrangement of chains with a direct AFM IC as modelled by four chains with $N = 24$ sites in each chain for different IC $j_{ic} \equiv J_{ic}/|J_1|$ and an inchain frustration $\alpha = 1/2$. Note that each point shown represents a step. The critical value of $\tilde{j}_{ic}/2$ amounts 0.088 for $D=3$ and 0.094 for $D=2$.

[12]. The small 1D-value of $H_s \approx 4.2$ to 5.9 T, only, clearly shows the importance of J_{ic} in the vicinity of the critical point where $H_s \rightarrow 0$. The validity of Eq. (2) is guaranteed by $j_{ic} = 0.0264756$ (i.e. 7.2 K) to 0.023659 (i.e. 6.5 K) exceeding well $j_{ic,cr} = 0.009539$ to 0.013458 deduced from the 2D-phase diagram. The $j_{ic,cr}$ would allow $H_s = 6.2$ T to 8.9 T in the triatic phase at most. The estimated weak IC given above is close to L(S)DA+ U results [14]. Thus, we are clearly outside the triatic or quartic phases and deep enough in the usual dipolar phase. The 1-magnon picture holds also for $\text{Li}(\text{Na})\text{Cu}_2\text{O}_2$ where $j_{ic,cr}$ for the nematic phase is exceeded by a factor of four. In fact, from the LDA derived J_{ic} and J_1 we estimate $j_{ic} \approx 0.7$ well above 0.170 $j_{ic,cr} = 0.1704$ taken from Fig. 2 for $\alpha \approx 1$ for LiCu_2O_2 [28]. Similarly, using the empirical values for NaCu_2O_2 : $\Theta_{CW} = -41$ K taken from the $1/\chi(T)$ data at $350 \leq T \leq 400$ K, $\alpha = 1.9$, $J_1 \approx -48$ K, and $g_a = 2.06$, we predict $H_s \sim 155$ T. From Eq. (1) we estimate $j_{ic} \sim 0.73$ well above $j_{ic,cr} \approx 0.172$ (see Fig. 2) and again close to LDA-results [30].

Now we turn to the case of diagonal IC as in Li_2CuO_2 (see Fig. 1). For a strong enough IC the MBS are suppressed and only 1-magnon excitations survive at high fields (see Fig. 4(b)). Then h_s reads

$$h_s = g\mu_B H_s/|J_1| = \tilde{j}_{ic} + \tilde{j}'_{ic} \text{ if } j_{ic} \geq j_{ic,1}^{\text{cr}}, \quad \tilde{j}_{ic} = N_{ic}j_{ic} \quad (6)$$

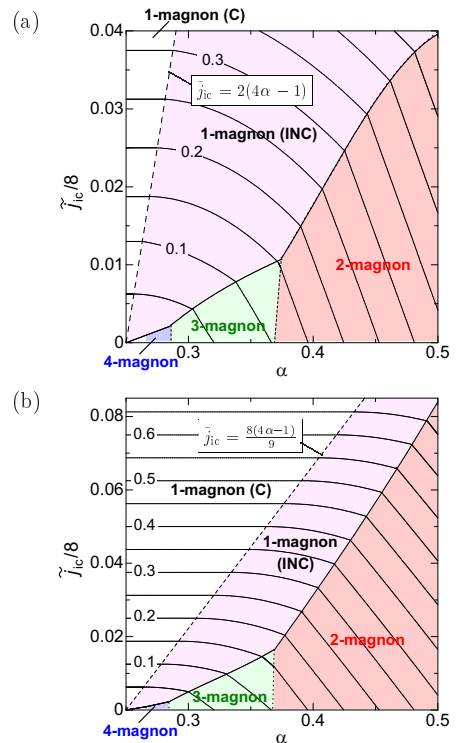


FIG. 4: (Color) 3D phase diagrams for diagonal IC. h_s (given by contour lines) as a function of the normalized IC \tilde{j}_{ic} and the inchain frustration α . Lower(Upper): (un)shifted chains with $\pm 3b/2$ ($\pm b$) IC, where b is the inchain Cu-Cu distance.

where $N_{ic} = 8$. Eq. (6) is valid for $j_{ic}(\alpha) > (4\alpha - 1)/9 \equiv j_{ic,1}^{cr}$ for $j'_{ic} = 0$. We obtained from INS data [17]: $J_{ic} \approx 9\text{K} > J_{ic,1}^{cr}(0.332) = -0.0364J_1 \approx 8.2\text{K}$. Then H_s depends *solely* on the IC which can be directly read off from $H_s(T = 0)$ [18]. For weaker IC h_s depends also somewhat on α . Our results also suggest that in this intermediate INC-phase above a second critical IC $j_{ic,2}^{cr} \approx 0.0109$ only specific INC 1-magnon low-energy excitations exist, see Fig. 4. Below $j_{ic,2}^{cr}$ 3-MBS are recovered as low-energy excitations and only this narrow region is 1D-like. The commensurate (C) phase behaves like an ordinary 3D antiferromagnet despite its seemingly quasi-1D nature. For unshifted NN chains (see Fig. 1), the C-phase is missing. There is only one critical IC separating INC 1-magnon excitations from 3-MBS.

Generally, $\theta = -2\Theta_{cw}/J_1$ provides a useful constraint

$$1 = \alpha + \beta + \theta + (D - 1)[j_{ic,\perp} + 2 \sum_f j_{ic,f}], \quad (7)$$

for the exchange integrals, where in addition to α further inchain and IC quantities $\beta = -J_3/J_1$, $j_{ic,\perp} = -J_{ic,\perp}/J_1$, and $j_{ic,f} = -J_{ic,f}/J_1$ for various diagonal couplings have been introduced. From Eq. (7) a stringent constraint for α for LiVCuO_4 follows. From $1/\chi(T)$ at $500\text{K} \leq T \leq 650\text{K}$ a small *FM* value $\Theta_{cw} = 7.4\text{K}$ can be fitted from the data shown in Refs. 25, 33. The *FM* ordering of spirals observed by neutron diffraction can be maintained both by a *FM* inplane and a perpendicular *AFM* 3D IC (see Fig. 1) Then we may assume for the sake of simplicity that both IC almost cancel in Eq. (7) and ignore the small terms β , and j_{ic} in zeroth approximation. The weakness of the total IC is suggested also by the weak magnetic moment $m = 0.3\mu_B$ at $T=0$ [34] pointing to strong quantum fluctuations. A first estimate [33] of the dispersion of the INS peaks as well as of the INS intensity above 10 meV yields a reasonable description for $\alpha=0.8$ and $J_1=-73.2\text{K}$ and $J_3=-0.07\text{K}$ as suggested by a mapping of a five-band Hubbard model (exact diagonalizations) for a Cu_6O_{12} cluster onto a six-site J_1 - J_2 - J_3 -Heisenberg ring. Hence, we conclude, that for $\alpha \approx 0.85 \pm 0.1$ and $J_1 \approx -80\text{K}$ nematics could be observed in LiVCuO_4 . Using Eq. (3) we see that this is also in reasonable accord with the experimental H_s -data [20, 25] since our 1D set gives for the above mentioned rough estimate about 48 T for $g = 2$ and H directed along the hard axes and about 42 T for the weak axis with $g = 2.3$. Note that our J 's differ strongly from those given inappropriately in Refs. 25, 26. The latter have been employed unfortunately in Refs. 6, 20 as 'empirical' input parameters. More detailed studies including explicitly the IC are necessary to refine all J 's. In particular, the quantum effect of J_{ic} on the pitch angle is of interest. A more detailed study of *FM* IC as well as of the J_1 - J_2 - J_3 inchain model will be considered elsewhere. A challenging point is also to find MP phases *beyond* the 2-magnon Bose condensation [6] triggered by a *FM* IC.

To summarize, the crucial role of realistic *AFM* IC in Q-1D helimagnets has been demonstrated. The rich and exotic physics of multipolar phases recently predicted for single chains is very sensitive to the strength of the IC. It can be readily eliminated by a weak *AFM* IC especially for triatic, quartic, etc. phases. For most CuO_2 chain systems studied so far, except probably LiVCuO_4 , where a nematic phase or some other exotic phase might be expected, the *AFM* IC is too strong to allow for multipolar phases. The examination of various weak *FM* IC as well as of anisotropy effects in real materials is under study.

We thank the DFG [grants DR269/3-1 (S-LD, SN), RI615/16-1 (JR) and the PICS program (Contr. CNRS No. 4767, NASU No. 243) [ROK] for support.

-
- [*] Corresponding author: s.l.drechsler@ifw-dresden.de
 - [2] S.-L. Drechsler *et al.*, *J. Magnet. & Magnet. Mat.* **290**, 345 (2005), -, *ibid.* **316**, 306 (2007).
 - [3] L. Kecke *et al.* *Phys. Rev. B* **76**, 060407 (2007).
 - [4] T. Hikihara *et al.*, *ibid.* **78**, 144404 (2008).
 - [5] J. Sudan *et al.*, *ibid.* **80**, 140402(R) (2009).
 - [6] M. Zhitomirsky and H. Tsunetsugu, arXiv:1003.4096v1.
 - [7] MBS appear at $H = 0$ also in Ising-type anisotropic 2D systems, ladders and other systems. See e.g.: C.J. Hamer, *Phys. Rev. B* **79**, 212413 (2009), S. Dusuel *et al.*, *ibid.* **81**, 064412 (2010) and references therein. Related aspects for frustrated chain cuprates will be considered elsewhere.
 - [8] R. Bursill *et al.*, *J. Phys.: Cond. Mat.* **7**, 8605 (1995).
 - [9] T. Vekua *et al.*, *Phys. Rev. B* **76**, 174420 (2007).
 - [10] F. Heidrich-Meisner *et al.*, *ibid.* **74**, 020403R (2008).
 - [11] D. Dmitriev *et al.*, *Phys. Rev. B* **79**, 054421 (2009).
 - [12] S.-L. Drechsler *et al.*, *Phys. Rev. Lett.* **98**, 077202 (2007).
 - [13] M. Sato *et al.*, *Phys. Rev. B* **79**, 060406(R) (2009).
 - [14] M. Schmitt *et al.*, *ibid.* **80**, 205111 (2009).
 - [15] R. Kuzian and S.-L. Drechsler, *ibid.* **75**, 024401 (2007).
 - [16] R. Zinke *et al.*, *ibid.* **79**, 094425 (2009).
 - [17] W.E.A. Lorenz *et al.*, *Europhys. Lett.* **88**, 37002 (2009).
 - [18] S. Nishimoto *et al.*, arXiv:1004.3300 (2010).
 - [19] N. Buettgen *et al.*, *Phys. Rev. B* **81**, 052403 (2010).
 - [20] L.E. Svistov *et al.*, arXiv:1005.5668v1
 - [21] M. Härtel *et al.*, *Phys. Rev. B* **78**, 174412 (2008).
 - [22] J. Sirker, *ibid.* **81**, 014419 (2010).
 - [23] H. Katsura *et al.*, *Phys. Rev. Lett.* **101**, 187207 (2008).
 - [24] H.T. Ueda and K. Totsuka, *Phys. Rev. B* **80**, 014417 (2009). Here J_{ic}^{\perp}/J_2 vs. $-1/\alpha$ has been plotted; note that in this plot its maximum occurs at $-1/\alpha \approx -1.67$.
 - [25] M. Enderle *et al.*, *Europhys. Lett.* **70**, 237 (2005).
 - [26] M. Enderle *et al.*, *Phys. Rev. Lett.* **104**, 237207 (2010).
 - [27] We prepare the first notation to underline its cuprate character at variance with the standard chemical notation with increasing charge of cations.
 - [28] A.A. Gippius *et al.*, *Phys. Rev. B* **70**, 020406(R) (2004).
 - [29] T. Masuda *et al.*, *Phys. Rev. B*, **72**, 014405 (2005).
 - [30] S.-L. Drechsler *et al.*, *Europhys. Lett.* **73**, 83 (2006).
 - [31] S.R. White, *Phys. Rev. Lett.* **69**, 2863 (1992).
 - [32] Y. Skourski (unpublished).
 - [33] S.-L. Drechsler *et al.*, arXiv:1006.5070.
 - [34] B.J. Gibson *et al.*, *Physica B* **350**, Suppl. e253 (2004).

Note that the ordered moment for LiVCuO_4 is three times smaller than that for Li_2CuO_2 or $\text{Ca}_2\text{Y}_2\text{Cu}_5\text{O}_{10}$.